Neurobiology of Aging 106 (2021) 119–129

Contents lists available at ScienceDirect

Neurobiology of Aging

journal homepage: www.elsevier.com/locate/neuaging.org

Unique regional patterns of amyloid burden predict progression to prodromal and clinical stages of Alzheimer's disease

Julia Pfeil[a,*], Merle C. Hoenig[a,b], Elena Doering[a,c], Thilo van Eimeren[a,c,d], Alexander Drzezga[a,b,c], Gérard N. Bischof[a], for the Alzheimer's Disease Neuroimaging Initiative

[a] Department of Nuclear Medicine, Multimodal Neuroimaging Group, University of Cologne, University Hospital of Cologne, Cologne, Germany
[b] Research Center Juelich, Institute for Neuroscience and Medicine II, Molecular Organization of the Brain, Juelich, Germany
[c] German Center for Neurodegenerative Diseases, Bonn/Cologne, Germany
[d] University of Cologne, University Hospital of Cologne, Department of Neurology, Cologne, Germany

ARTICLE INFO

Article history:
Received 25 February 2021
Revised 22 May 2021
Accepted 15 June 2021
Available online 21 June 2021

Keywords:
Alzheimer's disease
Mild cognitive impairment
Regional amyloid burden
Positron emission tomography
Disease progression
Amyloid-beta

ABSTRACT

Although beta-amyloid (Aβ) positivity has shown to be associated with higher risk of progression to Alzheimer's disease (AD) in mild cognitive impairment (MCI), information on the time to conversion to manifest dementia cannot be readily deduced from this binary classification. Here, we assessed if regional patterns of Aβ deposition measured with ^{18}F-florbetapir may serve as biomarker for progression risk in Aβ-positive cognitively normal (CN) and MCI patients, including clinical follow-up data and cerebrospinal fluid (CSF) biomarkers. Voxel-wise group comparisons between age and sex-matched Aβ-positive groups (i.e., CN-stables [n = 38] vs. CN-to-MCI/AD progressors [n = 38], MCI-stables [n = 104] versus MCI-to-AD progressors [n = 104]) revealed higher Aβ burden in precuneus, subcortical, and parietal regions in CN-to-MCI/AD progressors and cingulate, temporal, and frontal regions in MCI-to-AD progressors. Importantly, these regional patterns predicted progression to advanced stages on the AD spectrum in the short and the long-term beyond global Aβ burden and CSF biomarkers. These results suggest that distinct regional patterns of Aβ burden are a valuable biomarker for risk of disease progression in CN and MCI.

1. Background

The earliest pathological hallmark of Alzheimer's disease (AD) is the accumulation of amyloid-beta (Aβ). Even though Aβ accumulation may be evident in individuals more than 20 years before progression to clinical dementia (Bateman et al., 2012; Rowe et al., 2010), no overt symptoms are present at this point. Since clinical trials targeting Aβ accumulation at clinical stages of the disease have mostly failed so far, the need for new treatment approaches and diagnostic tools to identify individuals at an early, preclinical stage of the disease trajectory is high.

Positron emission tomography (PET) Aβ-tracers selectively bind to Aβ plaques, allowing the visualization and quantification of Aβ burden in the brain non-invasively. The clinical standard currently is still a binary distinction of individual patients into Aβ-positive or negative based on the global Aβ burden. Although a binary distinction is imperative for the differential diagnosis, additional information could be extracted from Aβ PET images that may potentially inform disease trajectories. Already post-mortem pathologic studies showed that Aβ deposition follows a specific pattern of spread (Thal et al., 2002). However, the predictive power of these regional associations concerning disease progression from prodromal to clinical stages remains to be elucidated. Regional Aβ burden in the posterior cingulate, precuneus, and lateral parietal, as well as the banks of the superior temporal sulcus has been associated with longitudinal cognitive decline in amyloid-negative cognitively normal elderly adults (Guo et al., 2020; Farrell et al., 2018), emphasizing the contribution of regional Aβ to cognitive aging. Nevertheless, these studies do not allow inferences about the role of regional Aβ burden of disease progression in preclinical or prodromal populations. Global Aβ burden, on the other hand, has been shown to predict progression to AD in some cases (Ciarmiello et al., 2019; Jun et al., 2019), however, the time of

* Corresponding author at: J. Pfeil, University of Cologne, University Hospital of Cologne, Department of Nuclear Medicine, Multimodal Neuroimaging Group, Kerpenerstraße 62, Cologne 50931, Germany. Tel.: +49 221 478 7503.
E-mail address: julia.pfeil@uk-koeln.de (J. Pfeil).

0197-4580/$ – see front matter
https://doi.org/10.1016/j.neurobiolaging.2021.06.014

progression to manifest dementia cannot be deduced from this binary classification or global measurement, so far. Nonetheless, this information would be essential from a clinical point of view, but also for the arrangement of patient's and care-taker's health-related matters.

We hypothesize that that specific regional patterns of Aβ deposition may constitute a predictive value for both Aβ-positive cognitively normal (CN) individuals and individuals with mild cognitive impairment (MCI) who subsequently advance on the continuum of clinical Alzheimer's disease (AD). Additionally, we propose that the regional susceptibility of Aβ to predict progression is different depending on the baseline diagnosis (i.e., CN or MCI). Lastly, we hypothesize that this potential identified pattern of regional Aβ may constitute a more predictive biomarker than global Aβ or CSF measures, and that they may be unique for disease progression stage.

2. Methods

2.1. Participants

Data used for this study were derived from the Alzheimer's Disease Neuroimaging Initiative (ADNI) (http://adni.loni.usc.edu/). Key screening criteria for inclusion were: (1) Aβ-positivity from baseline until follow-up (standardized uptake value ratio (SUVR) $>$ 1.1, see Landau & Jagust (2015) for assessment of this measure), (2) availability of an ^{18}F-Florpetapir PET scan at baseline, (3) a diagnosis of either cognitively normal or mild cognitive impairment at baseline, and (4) a follow-up diagnosis (at least 6 months from baseline) of either CN, MCI, or AD. The clinical diagnosis of Alzheimer's disease was based on the recommended diagnostic National Institute on Aging and Alzheimer's Association (NIA-AA) guidelines from 2011 (Albert et al., 2011; Jack Jr et al., 2011; McKhann et al., 2011; Sperling et al., 2011). This resulted in 284 participants, 168 males and 116 females (mean age 74.7 $\pm$ 6.5 years), out of which 4 groups were defined: (1) individuals who were cognitively normal at baseline and remained stable over a period of at least 6 months (CN-CN), (2) individuals who were cognitively normal and progressed to MCI or AD (CN-MCI/AD), (3) individuals with a baseline diagnosis of MCI, who remained stable over a time period of at least 6 months (MCI-MCI), and (4) individuals with a baseline diagnosis of MCI who progressed to AD (MCI-AD). The CN-CN and CN-MCI/AD groups and the MCI-MCI and MCI-AD groups were matched on age and sex, respectively. Furthermore, it was ensured that each progressed participant was matched with a participant who remained stable for at least the same amount of time their matched progressor stayed stable.

2.2. Positron emission tomography (PET)

All participants underwent a PET-scan with the ^{18}F-florbetapir PET tracer. Participants received an average dosage of 370 MBq (10 mCi) of ^{18}F-florbetapir with 20 minutes (4 $\times$ 5 minutes frames) acquisition at 50–70 minutes post-injection (for more information see http://adni.loni.usc.edu/methods/pet-analysis-method/pet-analysis/).

2.3. CSF measures

Most participants underwent a lumbar puncture to measure baseline amyloid-beta 1-42 peptide (CSF Aβ), total tau (CSF t-tau), and tau phosphorylated at the threonine 181 (CSF p-tau). Out of 286 participants, 228 had a CSF Aβ measure and 233 had a CSF t-tau as well as aCSF p-tau measure. Lumbar puncture was performed with a 20-24-gauge spinal needle as described in the ADNI procedures manual (http://www.adni-info.org/).

2.4. Imaging data pre-processing

PET data was pre-processed with Statistical Parametric Modeling 12 (SPM12, Wellcome Trust Center, www.fil.ion.ucl.ac.uk/spm) implemented in Matlab 2019b (Mathworks Inc., Sherborn, MA). All PET images were aligned to the anterior-posterior commissure and spatially normalized to the tissue probability map implemented in SPM12. Then, all images were smoothed with an 8 mm FWHM Gaussian filter, as this has been found to be an appropriate value to use (Tsutsui et al., 2018) and has been employed frequently in previous studies (Lin et al., 2016; Saint-Aubert et al., 2013; Teipel et al., 2015). Lastly, SUVRs for the images were computed by using the whole cerebellum as reference region.

A global Aβ score, previously published (details for preprocessing see Landau & Jagust, 2015), was used, which was derived by taking the fully processed ^{18}F-florbetapir scans and co-registering and normalizing them to its corresponding MRI-image that was closest in time to that scan. All MRI images were skull-stripped, segmented, and delineated into cortical and subcortical regions. ^{18}F-florbetapir SUVr means were extracted from grey matter in each subregion within 4 cortical regions (frontal, anterior/posterior cingulate, lateral parietal, and lateral temporal regions) using the whole cerebellum as reference region. Finally, a composite global Aβ SUVr score was computed based on the 4 cortical regions.

2.5. Statistical analysis

Non-parametric (i.e., Mann-Whitney-U-tests; Pearson-Chi-Square-tests) tests were performed to compare the groups on age, sex, years of education, Apolipoprotein E4 (APOE4) carriership, and baseline values of global Aβ burden, CSF Aβ, CSF t-tau, and CSF p-tau. To assess regional differences in Aβ burden between the stable and progressor groups, 2-sample t-tests were performed in SPM12 comparing the CN-CN group against the CN-MCI/AD group and the MCI-MCI group against the MCI-AD group, respectively. APOE4 carriership was entered as covariate. To reduce the number of voxel-wise comparisons, a brain mask with all regions of the AAL atlas, except for the cerebellum, was included in the analyses. Subsequently, significant regions were extracted and saved in a binarized format in MNI space. SUVRs of all participants were extracted from these regions and the overall mean across regions was computed. Binary logistic regression analyses were performed to quantify the effect of regional Aβ burden over all other variables of interest (age, sex, education, APOE4 carriership, global Aβ burden, and all 3 CSF measures) in the prediction of progression. For this, all predictor variables were entered simultaneously into the regression model together with regional Aβ burden.

To assess whether regional Aβ burden extracted from one of the respective groups (CN or MCI) is predictive of progression in the other group, additional logistic regression analyses were performed, including the mean regional SUVRs from the other respective groups and all other predictors from the previous analyses. Again, all predictor variables were entered in the regression model simultaneously. For the CN-CN versus CN-MCI/AD groups, 27 progressors and 28 stables were included in the analyses due to missing data points for some variables, while for the MCI-MCI versus MCI-AD groups, 74 progressors and 99 stables were included. Finally, multinomial logistic regression analyses were performed comparing fast against slow progressors in both the CN-MCI/AD group and the MCI-AD group, respectively (Appendix A1, Tables A1–3). All analyses were performed using SPSS 25.0.

Table 1
Mean and standard deviations per group and variable

Variable	CN-CN(N = 38)	CN-MCI/AD(N = 38)	MCI-MCI(N = 104)	MCI-AD(N = 104)
Age (y)	78.05 ± 5.31	78.33 ± 5.38	73.57 ± 6.43	73.30 ± 6.53
Sex (m/f)	20/18	20/18	63/41	63/41
APOE4 (±)	8/30	21/17	63/41	78/26
Education (y)	16.71 ± 2.23	16.29 ± 2.89	16.24 ± 2.92	16.32 ± 2.63
Months stable	60.32 ± 25.03	28.84 ± 24.15	43.15 ± 23.43	27.75 ± 19.98
CSF Aβ	1018.78 ± 419.75 (28)	830.49 ± 354.30 (27)	800.86 ± 269.04 (74)	682.40 ± 184.59 (99)
CSF t-tau	306.33 ± 13.05 (28)	303.89 ± 91.11 (27)	287.59 ± 116.33 (79)	374.62 ± 137.40 (99)
CSF p-tau	29.54 ± 13.67 (28)	29.85 ± 10.45 (27)	27.42 ± 11.75 (79)	37.98 ± 15.92 (99)
Global Aβ	1.25 ± 0.19	1.34 ± 0.18	1.33 ± 0.18	1.44 ± 0.16

Values are given as mean ± standard deviation. Values in brackets are number of included data points if data was missing.
Key: APOE4, Apolipoprotein E4; CN-CN, cognitively normal stable; CN-MCI/AD, cognitively normal progressed to MCI or AD; MCI-MCI, mild cognitive impairment stable; MCI-AD, mild cognitive impairment progressed to AD.

Table 2
Group Differences between CN-CN versus CN-MCI/AD and MCI-MCI versus MCI-AD

	Mean rank CN-CN	*N*	Mean rank CN-MCI/AD	*N*	*U* / X^2	***Z***	$\boldsymbol{n^2}$
Months being stable	47.21	38	29.79	38	391.000[b]	-3.495	-0.83
Global Aβ	31.87	38	45.13	38	470.000[a]	-2.618	-0.90
APOE4 (±)	-	8/30	-	21/17	9.432[a]	-	-
	MCI-MCI		MCI-AD				
Months being stable	125.06	104	83.94	104	3269.500[b]	-4.992	-0.88
Global Aβ	83.56	104	125.44	104	3230.000[b]	-5.018	-0.87
CSF Aβ	100.01	74	77.27	99	2700.000[a]	-2.955	-0.85
CSF t-tau	69.47	79	105.48	99	2328.500[b]	-4.632	-0.85
CSF p-tau	67.92	79	106.72	99	2205.500[b]	-4.992	-0.95
APOE4 (±)	-	63/41	-	78/26	4.954[a]	-	-

Mann-Whitney-U-Tests and Pearson-Chi Square-Tests for CN-CN versus CN-MCI/AD, and MCI-MCI versus MCI-AD groups. Data showing non-significant associations was omitted from the table.
Key: APOE4, Apolipoprotein E4; CN-CN, cognitively normal stable; CN-MCI/AD, cognitively normal progressed to MCI or AD; CSF, cerebrospinal fluid; MCI-MCI, mild cognitive impairment stable; MCI-AD, mild cognitive impairment progressed to AD; P-tau, Phospho-tau; T-tau, total-tau.
[a] $p < 0.05$.
[b] $p < 0.001$.

2.6. Sensitivity analysis

To investigate whether the matching procedure based on follow-up timepoints (i.e., MCI-MCI with 2 years follow-up was matched to MCI-AD with 2 years follow-up) might have influenced our analyses, a sensitivity analysis was performed. For this, participants in the stable groups (CN-CN and MCI-MCI) were selected if they were stable for at least 4 years, while participants in the progressor groups (CN-MCI/AD and MCI-MCI) were selected if they progressed within 3 years of the ^{18}F-Florpetapir PET baseline scan. The follow-up time periods were chosen to maximize time and group size. The approach mimicked the analysis described in 2.5 (Appendix B1, Table B1, Figure B1).

3. Results

3.1. Group characteristics

Mean and standard deviations are reported (Table 1). At baseline, the CN-CN and CN-MCI/AD groups were of similar age, years of education, ratio of females to males, CSF Aβ, CSF t-tau, and CSF p-tau. The MCI-MCI and MCI-AD groups were of similar age, years of education, and ratio of females to males. The CN-MCI/AD group showed a higher global Aβ burden at baseline than the CN-CN group ($p = 0.009$). The CN-CN group showed an increased number of months of clinical stability ($M_{CN\text{-}CN} = 60.32$, $M_{CN\text{-}MCI/AD} = 28.84$, $p < 0.001$) and included more APOE4-negative individuals ($p = 0.002$) than the CN-MCI/AD group. Similarly, the MCI-MCI group included more APOE-negative individuals than the MCI-AD group ($p = 0.026$). The MCI-AD group showed a reduced number of months of clinical stability ($M_{MCI\text{-}MCI} = 43.15$, $M_{MCI\text{-}AD} = 27.75$, $p < 0.001$), a larger global Aβ burden ($p < 0.001$), CSF Aβ ($p < 0.001$), CSF t-tau ($p < 0.001$), and CSF p-tau ($p < 0.001$) than the MCI-MCI group (Table 2).

3.2. Regional differences in Aβ burden

The voxel-wise whole-brain analysis yielded higher regional Aβ burden in the left and right precuneus, right lingual and angular gyrus, putamen, caudate, pallidum, middle temporal gyrus, and superior temporal gyrus for the CN-MCI/AD group compared to the CN-CN group ($p < 0.001$, uncorrected, Fig. 1A). None of the clusters in this comparison survived correction for multiple comparisons. Regional Aβ burden was also higher in the left and right anterior cingulate gyrus, medial frontal cortex, precuneus, right transverse temporal gyrus, left middle and superior temporal gyrus, posterior and anterior insula, central operculum, and medial segment of the superior frontal gyrus for the MCI-AD group compared to the MCI-MCI group (FWE-corrected, Fig. 1B). Upon visual assessment, hemispheric asymmetry was observed, shifting from right (higher Aβ burden in the right hemisphere in CN) to left (higher Aβ burden in the left hemisphere in MCI) depending on the disease stage (i.e., CN or MCI).

3.3. Predictive factors of progression

Results indicated that regional Aβ was predictive for progression from CN to MCI and AD, whereas all other predictors, including global Aβ burden, were not ($X^2(9) = 21.029$, $p = 0.013$). APOE4 carriership was trend significant in the model ($p = 0.051$).

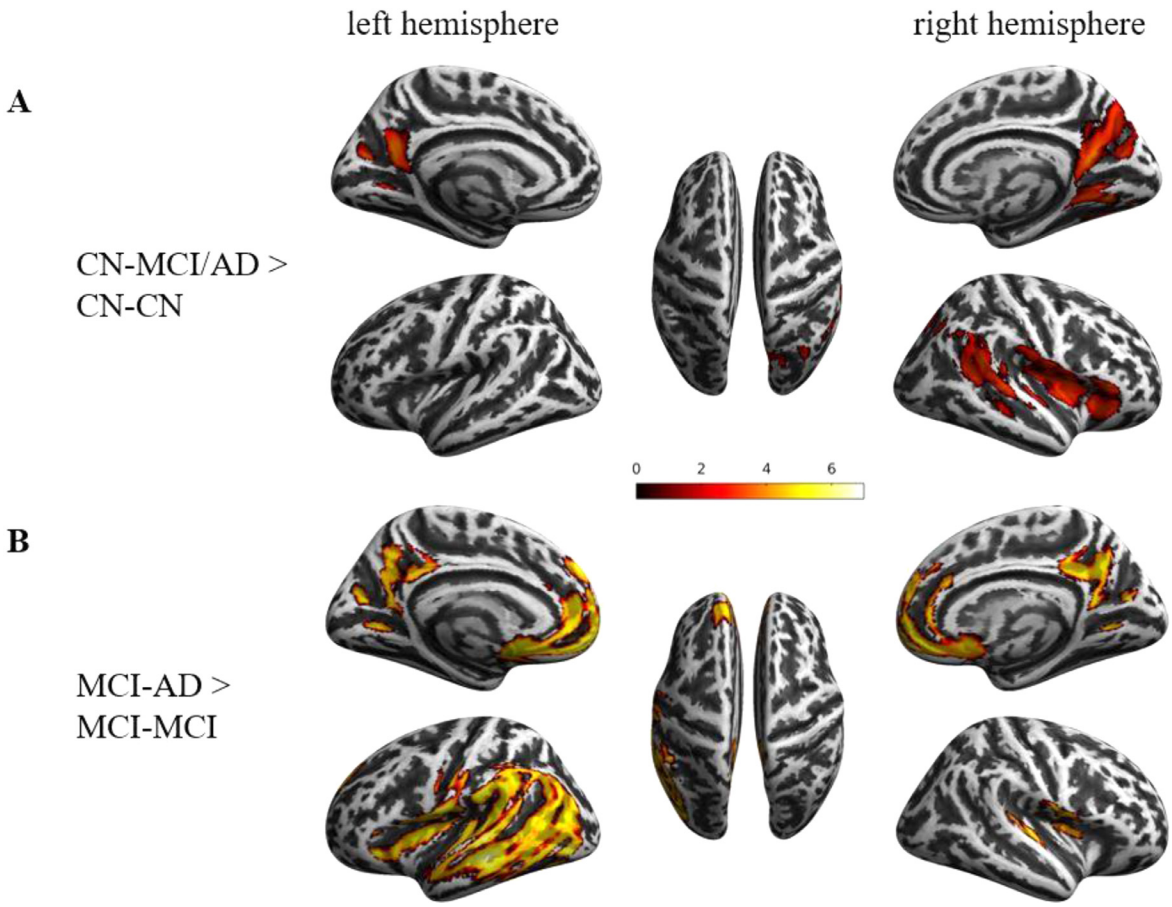

Fig. 1. Regional differences in Aβ burden. (A) Regional differences in Aβ burden for CN-MCI/AD (N = 38) > CN-CN (N = 38), and (B) MCI-AD (N = 104) > MCI-MCI (N = 104). Results are color-coded according to the t-value statistics and illustrated on an inflated representation of the brain using CAT12 toolbox.

Table 3
Binary logistic regression analysis for variables predicting progression from CN to MCI or AD and from MCI to AD

	Predictor	β	SE β	Wald's X^2	*df*	*p*	e^{β}
CN-CN versus	Constant	-15.390	7.833	3.860	1	0.049	0.000
CN-MCI/AD	Regional Aβ	5.013	1.865	7.221	1	0.007	150.333
MCI-MCI versus	Constant	-7.347	3.111	5.577	1	0.018	0.001
MCI-AD	CSF Aβ	-0.002	0.001	4.731	1	0.030	0.998
	Regional Aβ	9.834	3.551	7.670	1	0.006	18650.596
	Test			X^2	*df*	*p*	Nagelk. R^2
CN-CN versus	Overall model evaluation			21.029	9	0.013	0.424
CN-MCI/AD	Goodness-of-fit test			10.282	7	0.173	-
MCI-MCI versus	Overall model evaluation			51.686	9	0.000	0.347
MCI-AD	Goodness-of-fit test			6.333	8	0.610	-

All predictor variables that showed non-significant associations were omitted from the table.
CN-CN n = 27, CN-MCI/AD n = 28. MCI-MCI n = 99, MCI-AD n = 74.
Key: e^{β}, odds ratio. CI, confidence interval.

The model explained 42.4% of the variance and correctly classified 80.0% of cases (Table 3). For the full results table see Appendix C. Regional Aβ and increased age were particularly sensitive to predict progression in fast ($\leq$ 36 months) compared to slow (>36 months) progressors. APOE4 carriership, on the other hand, was particularly sensitive to predict progression in slow compared to fast progressors (Appendix A1).

For the MCI-MCI versus MCI-AD comparison, the CSF Aβ score and the mean regional SUVR were significant in the model ($X^2(9) = 51.686$, $p < 0.000$), indicating that a higher CSF Aβ score and higher Aβ burden in the identified regions are predictive for progression from MCI to AD. The model explained 34.7% of variance and correctly classified 74.6% of cases (Table 3). Regional Aβ predicted conversion within 12 months after established Aβ-positivity, together with sex and APOE4 carriership ($X^2(18) = 57.095$, $p < 0.001$). None of the variables predicted slow conversion (Appendix A1).

3.4. Analyzing the unique regional pattern of Aβ burden as a predictor of disease progression

We evaluated if the mean SUVRs in the regional cluster identified in the CN-CN versus CN-MCI/AD comparison was also sensitive in the regression model to predict MCI-AD progression. This model only yielded a significant effect of CSF Aβ ($X^2(9) = 43.022$, $p < 0.001$), while all other predictors were not significant. When

the reverse analysis was performed including the CN-CN and CN-MCI/AD groups with the mean SUVR of the identified regions from the MCI-MCI versus MCI-AD analysis, none of the variables were significant in the model. Results indicate that the identified regions of the 2 comparisons are both unique for predicting progression from and to specific disease stages. The sensitivity analysis only including individuals with at least 4 years of follow-up revealed a similar regional pattern, but the variance explained by this model increased by 20% (Appendix B1).

4. Discussion

The main results of this study showed that specific regional Aβ deposition patterns predict progression from CN to MCI or AD, as well as progression from MCI to AD. In addition to known predictors such as APOE4 carriership and age, the regional pattern of Aβ burden was predictive for more rapid progression from CN to MCI or AD within 3 years after established Aβ-positivity. Similarly, regional Aβ burden was predictive for fast conversion from MCI to AD within one year after established Aβ-positivity, together with sex and APOE4 carriership. Finally, Aβ regions identified in each group comparison were unique for the prediction of progression within each progressor group (i.e., CN to MCI/AD or MCI to AD) and were confirmed with an additional sensitivity analysis. Results demonstrate that regional Aβ constitutes a valuable predictor for progression to prodromal and clinical AD in Aβ-positive individuals, which had more predictive value than global Aβ or single CSF biomarkers. Findings are discussed in more detail in the context of (1) regional Aβ staging, (2) hemispheric asymmetry, and (3) the contribution of APOE4 carriership and CSF biomarkers.

4.1. Regional Aβ staging: Unique regional patterns of Aβ predict progression

Recent studies investigating regional Aβ burden explored its topographical pattern in vivo using Aβ-PET (Cho et al., 2016; Grothe et al., 2017; Mattsson et al., 2019; Sakr et al., 2019) and observed successive Aβ accumulation beginning in the precuneus, medial orbitofrontal and posterior cingulate cortices, spreading to core regions of the default mode network, associative neocortex, primary sensory-motor cortex, and medial temporal lobe, finally affecting the striatum. Here, we demonstrate that beyond global Aβ burden, Aβ accumulation in precuneus, lingual and angular gyrus, medial and superior temporal gyrus as well as subcortical regions was predictive of progression from a cognitively normal state to prodromal or clinical AD. Most of these regions are comprised in stage 1 of the staging model proposed by Mattsson and colleagues (Mattsson et al., 2019), suggesting that regions susceptible early in the process of Aβ deposition continue to accumulate Aβ and are indicative of disease progression. The identified regions and higher age were especially predictive for fast progression from CN to MCI or AD, that is, progression within the first 36 months after Aβ-positivity. The observed age effect is in line with previous studies reporting an increased risk of progression with advanced age (Corrada et al., 2010; Oulhaj et al., 2009). Furthermore, age-associated slowing of clearance mechanisms of Aβ has been suggested to be a factor of increased progression (Patterson et al., 2015). As our analyses have shown, the identified regions are unique for disease progression stage, despite some regional overlap (i.e., in the precuneus). The MCI-AD group showed a more widespread pattern of Aβ accumulation compared to the CN-MCI/AD group, demonstrating that regions such as the precuneus accumulate Aβ early and late during the disease progression, while regions such as the medial frontal cortex or anterior insula show increased Aβ accumulation only in advanced disease stages.

However, not all of the identified regions in our analyses matched the regional stage phase 1 reported by Mattsson's et al., (2019). These differences might be explained by different methodological approaches between the current study and the staging approach (Mattsson et al., 2019). Whereas Mattsson and colleagues (2019) used CSF and PET data to build composite regions of Aβ-staging, our study used different clinical diagnoses in addition to global measures of Aβ-positivity as main inclusion criteria (i.e., CN, MCI, AD) to identify regional differences. Overall, our study demonstrates the utility of regional Aβ deposition in the prediction of disease progression, similar to these previously presented staging approaches (Grothe et al., 2017; Mattsson et al., 2019). A study by Hanseeuw and colleagues (2018) included the striatum in their staging model and showed that the striatum is one of the last regions to accumulate Aβ while cortical regions start to accumulate Aβ first. In line with this, we were able to demonstrate that the striatum is a sensitive region for differentiating Aβ-positive CN-stables from CN-MCI/AD progressors. In later stages of the disease, other regions (i.e., anterior cingulate gyrus, medial frontal cortex, precuneus, transverse temporal gyrus, middle and superior temporal gyrus, posterior and anterior insula) seem to be more sensitive in differentiating Aβ-positive MCI-stables from MCI-AD progressors.

Our results suggest that a binary distinction in Aβ-positives and negatives might not be sufficient to inform on differential disease trajectories and therefore underscores the importance of considering additional regional susceptibilities in the clinical setting. Given our results, we propose that different magnitudes of Aβ burden in specific regions, as recently suggested (Bischof & Jacobs, 2019), could be utilized to examine the future course of the disease progression. Furthermore, our sensitivity analysis revealed mostly similar regional patterns of Aβ burden with our main analysis, indicating that the variability in follow-up length between progressors and non-progressors did not significantly influence the results.

Our results may have consequences for the clinical reading of Aβ-PET. In addition to assessing global Aβ burden visually, a regional reading approach using the identified cluster here, could potentially assist the clinician in evaluating a clinical prognosis for the patient. From a clinical point of view, prognosis and disease trajectories are the most frequent questions posed by caregivers and patients, therefore replicating these results is crucial from many perspectives.

4.2. Hemispheric asymmetry of Aβ deposition

Interestingly, when assessing the regional Aβ distribution patterns, a particular hemispheric dominance was observed dependent on progression type (i.e., CN-MCI/AD or MCI-AD). Here we showed that Aβ deposition appears to preferentially start in the right hemisphere in prodromal stages of the disease, ultimately spreading to regions in the left hemisphere with disease progression, suggesting that left-hemispheric Aβ accumulation is associated with cognitive decline. Most people show a left-hemispheric dominance, meaning that right-hemispheric pathology remains unnoticed for a longer time due to compensatory mechanisms of the left hemisphere. However, pathology does not have to start in the right hemisphere nor does right-hemispheric pathology reflect early disease stages. Left-hemispheric dominance of Aβ deposition may become symptomatic faster than right-hemispheric dominance. With this, it appears that left-hemispheric dominance of Aβ deposition is associated with advanced disease progression.

Aβ deposition follows a specific pattern of spread over time (Thal et al., 2002). To our knowledge, only few studies have reported a hemispheric asymmetry of Aβ deposition, among which a study by Frings and colleagues (Frings et al., 2015). They observed

a leftward asymmetry of Aβ associated with more severe cognitive impairment in language performance, while there was a rightward asymmetry of Aβ associated with decline in tasks involving visuospatial perception. The previous inability to detect this relationship has often been ascribed to a plateau of Aβ deposition, which has been reached while degeneration and the progression of cognitive deficits. This is mostly true for studies using post-mortem Aβ pathology and in vivo cognition, while the current study investigated both in vivo Aβ pathology and cognition. Our results on hemispheric asymmetry of Aβ deposition specifically highlight the advantage of in vivo studies and suggest that hemispheric asymmetry of Aβ may be a valuable biomarker in the future that needs further validation.

4.3. Contribution of APOE4 carriership and CSF biomarkers

Even though APOE4 carriership was only trend significant in the CN-CN versus CN-MCI/AD analysis, it was a significant predictor for progression after 3 years of Aβ-positivity. It is thought that APOE4 carriership is particularly associated with the accumulation and initial spread of Aβ across cortical regions (Kanekiyo et al., 2014). However, once Aβ has accumulated across the brain, APOE4 carriership may be less relevant for cognitive decline, and tau pathology or neurodegeneration subsequently become more prevalent (Morris et al., 2010). Accordingly, APOE4 carriership predicted slow progression from CN to MCI/AD, hence progression after 36 months of Aβ-positivity. Since APOE4 carriership is a long-life risk factor for AD, potential compensatory mechanisms to Aβ accumulation may have developed earlier in life in APOE4-carriers compared to non-carriers, thus explaining the generally slower trajectories to advanced disease stages in this cohort. Current evidence on the relationship of differential trajectories of cognitive decline and APOE4 carriership is mixed. Some studies suggest APOE4 carriership accelerates cognitive decline (Craft et al., 1998; Hirono et al., 2003), while others suggest APOE4 carriership decelerates cognitive decline (Frisoni et al., 1995; Stern et al., 1997). Yet, others report no significant effect of APOE4 carriership on cognitive trajectories (Kleiman et al., 2006). However, most of the studies investigating this relationship showed different methodological approaches or included different populations (i.e., early vs. late-onset AD patients), which could explain the mixed result pattern. Notably, our results suggest that processes leading to the onset of AD may differ from those that determine its clinical onset. APOE4 carriers may have a greater risk for AD but show a different effect on processes determining the rate of progression than APOE4 non-carriers.

Interestingly, none of the CSF variables was significant in predicting progression from CN to MCI or AD. However, among the CSF biomarkers, CSF Aβ predicted progression from MCI to AD in both our main and sensitivity analyses. This suggests that in vivo assessments of regional Aβ may be a better predictor for particularly short-term progression than single CSF measures of Aβ or tau, once individuals have reached Aβ-positivity. CSF markers turn positive earlier in the disease cascade than in vivo PET imaging, limiting their value for short-term prediction of clinical progression (Fagan et al., 2006; Fagan et al., 2009). In contrast, ratios of specific CSF biomarkers (i.e., Aβ42/Aβ40 or Aβ42/p-tau) were successful in predicting progression from prodromal to clinical AD, potentially suggesting that ratio information rather than single parameters derived from CSF have more predictive value, specifically in Aβ-positive individuals (Ferreira et al., 2014). Despite CSF measures being more easily available than in vivo PET imaging, our results have shown that Aβ PET is a more informative measure for the prognostic prediction of progression to MCI or AD than single CSF measures, especially in already Aβ-positive individuals.

4.4. Limitations and future directions

Some limitations of this study need to be mentioned. First, due to the use of publicly available data from the ADNI database, the analyses were limited to patients for whom a complete dataset for all the assessed predictive variables were available. Nevertheless, for the longitudinal design of our approach, and the holistic biomarker model we interrogated, the number of subjects is sufficient, but warrants replication in a different cohort, as well as using different fluorine labelled tracers for Aβ quantification. Nevertheless, we had the privilege to use this unique dataset, containing a variety of longitudinal data, whereas other datasets still need to advance to show a comparable sample size. Secondly, we used the same cohort for the extraction of regional Aβ patterns and the investigation of the utility of these regions in predicting progression to advanced disease stages. Therefore, future studies may want to use these findings to validate the predictive value of the identified regions in a different cohort. Also, we only included single CSF measures instead of ratio information due to missing data from the ADNI database. Inclusion of these could have resulted in more conclusive results on the contribution of CSF biomarker and should be addressed in future work. Thirdly, results regarding the asymmetry pattern observed when comparing Fig. 1A and B should be taken with caution, since they are not based on longitudinal follow-up analyses in the same individuals. Even though our study points towards this hemispheric asymmetry, more longitudinal studies are needed to validate these results. Lastly, ADNI represents a trial population, including primarily amnestic MCI patients, rather than a clinical heterogeneous cohort. Thus, constructing models for Aβ PET in ADNI might have resulted in an overestimation of the effect of Aβ PET as found in amnestic MCI patients. However, especially amnestic MCI patients may benefit from these results, as clinicians may be able to provide disease prognoses by evaluation of Aβ burden in the identified regions.

The current recommendation of Aβ-PET imaging does not suggest a clinical value for Aβ-positivity in asymptomatic individuals. However, our results have shown that Aβ-PET imaging is able to provide information on the imminent cognitive decline and trajectory in the short-and long run in even asymptomatic individuals (i.e., CN). Results may aid in identifying those Aβ-positive healthy individuals who are at an increased risk for progression and could potentially lead to a revision of the current diagnostic guidelines of Aβ-PET imaging.

4.5. Conclusion

Regional Aβ burden appears to be the most sensitive prognostic biomarker of progression in comparison to multiple other biomarkers in both Aβ-positive CNs and MCIs. These findings suggest that regional Aβ burden may aid in the future to assess the short-term prognostic trajectories for imminent cognitive decline in preclinical and prodromal patients on the AD continuum. Especially Aβ-positive healthy individuals may benefit from these results, as current Aβ-PET guidelines do not include this cohort as a target population.

Verification

As corresponding author, I take full responsibility for the data, the analyses and interpretation, and the conduct of the research. I had full access to all of the data and have the right to publish any data. All co-authors have seen and agreed to conditions noted on the Author Agreement Form. As per ADNI protocols, all procedures performed in studies involving human participants were in accordance with the ethical standards of the institutional and/or na-

tional research committee and with the 1964 Helsinki declaration and its later amendments or comparable ethical standards. More details can be found at adni.loni.usc.edu. (This manuscript does not contain any studies with human participants performed by any of the authors). The manuscript has not been previously published and is not under consideration for publication elsewhere. No submissions overlapping with the current work have previously been published.

Disclosure statement

The authors declare the following financial interests/personal relationships which may be considered as potential competing interests: JP, MCH, ED and GNB report no conflict of interest. TvE reports having received consulting and lecture fees from Lundbeck A/S, Lilly Germany, Shire Germany and research funding from the German Research Foundation (DFG), the Leibniz Association and the EU-joint program for neurodegenerative disease research (JPND). AD reports having received research support and speaker honoraria by Life Molecular Imaging, AVID/Lilly Radiopharmaceuticals, Siemens Healthineers, GE Healthcare.

Acknowledgements

GNB received funding from Alzheimer Forschung Initiative e.V., Germany (AFI K1707). In addition, this study was supported by the German Research Foundation (DFG, DR 445/9-1). This project has been partly funded by the Innovative Medicines Initiative 2 Joint Undertaking under Amyloid Imaging to Prevent Alzheimer's Disease (AMYPAD) grant agreement No. 115952. This communication reflects the views of the authors and neither IMI nor the European Union and EFPIA are liable for any use that may be made of the information contained herein. Data collection and sharing for this project was funded by the Alzheimer's Disease Neuroimaging Initiative (ADNI) (National Institutes of Health Grant U01 AG024904) and DOD ADNI (Department of Defense award number W81XWH-12-2-0012). ADNI is funded by the National Institute on Aging, the National Institute of Biomedical Imaging and Bioengineering, and through generous contributions from the following: AbbVie, Alzheimer's Association; Alzheimer's Drug Discovery Foundation; Araclon Biotech; BioClinica, Inc.; Biogen; Bristol-Myers Squibb Company; CereSpir, Inc.; Cogstate; Eisai Inc.; Elan Pharmaceuticals, Inc.; Eli Lilly and Company; EuroImmun; F. Hoffmann-La Roche Ltd and its affiliated company Genentech, Inc.; Fujirebio; GE Healthcare; IXICO Ltd.; Janssen Alzheimer Immunotherapy Research & Development, LLC.; Johnson & Johnson Pharmaceutical Research & Development LLC.; Lumosity; Lundbeck; Merck & Co., Inc.; Meso Scale Diagnostics, LLC.; NeuroRx Research; Neurotrack Technologies; Novartis Pharmaceuticals Corporation; Pfizer Inc.; Piramal Imaging; Servier; Takeda Pharmaceutical Company; and Transition Therapeutics. The Canadian Institutes of Health Research is providing funds to support ADNI clinical sites in Canada. Private sector contributions are facilitated by the Foundation for the National Institutes of Health (www.fnih.org). The grantee organization is the Northern California Institute for Research and Education, and the study is coordinated by the Alzheimer's Therapeutic Research Institute at the University of Southern California. ADNI data are disseminated by the Laboratory for Neuro Imaging at the University of Southern California.

Ethical approval

As per ADNI protocols, all procedures performed in studies involving human participants were in accordance with the ethical standards of the institutional and/or national research committee and with the 1964 Helsinki declaration and its later amendments or comparable ethical standards. More details can be found at adni.loni.usc.edu. (This article does not contain any studies with human participants performed by any of the authors).

Availability of data and material

Data used in preparation of this article were obtained from the Alzheimer's disease Neuroimaging Initiative (ADNI) database (http://adni.loni.usc.edu). Thus, the investigators within the ADNI contributed to the design and implementation of ADNI and/or provided data but did not participate in this analysis or the writing of this report. A complete listing of ADNI investigators can be found at http://adni.loni.usc.edu/wpcontent/uploads/how_to_apply/ADNI_Acknowledgement_List.pdf/.

Appendix A

A1. Fast versus slow progressor analyses

Since participant's time to progression varied from 6 up to 84 months, a post-hoc analysis was performed to determine differences in time to progression. For this, both the CN-MCI/AD group and the MCI-AD group were divided into a "fast" and a "slow" progressor group by a median split of the time being stable until progression, which yielded 36 months as median for the CN-MCI/AD group and 24 months as median for the MCI-AD group. Thus, participants progressing ≤36 months were included in the fast progressor group, while those progressing >36 months were included in the slow progressor group for the CN-MCI/AD analysis. Similarly, participants progressing <24 months were included in the fast progressor group, while those progressing >24 months were included in the slow progressor group for the MCI-AD analysis. This yielded a final dataset of 21 fast CN-MCI/AD progressors, 17 slow CN-MCI/AD progressors, and the initial 38 stables from the CN-CN group, as well as 35 fast MCI-AD progressors, 35 slow

Table A1
Group differences between fast and slow progressors

	Fast progressors Mdn (SD)	Slow progressors Mdn (SD)	Test stat/*p*
CN-MCI/AD			
Sex (m/f)	11/10	9/8	0.001/0.973[b]
APOE4 (±)	9/12	12/5	2.922/0.087[b]
Age	81.90 (4.81)	75.00 (4.22)	**59.000/0.000**[a,c]
Years of education	16.00 (2.89)	16.00 (2.96)	158.000/0.561[c]
Global Aβ	1.3 (0.16)	1.4 (0.20)	147.000/0.355[c]
CSF Aβ	793.30 (382.40)	747.00 (320.95)	75.500/0.486[c]
CSF t-tau	329.60 (102.79)	334.80 (78.43)	86.500/0.867[c]
CSF p-tau	33.37 (11.86)	30.32 (8.89)	85.500/0.829[c]
Regional Aβ	1.50 (0.24)	1.51 (0.21)	192.000/0.706[c]
MCI-AD			
Sex (m/f)	20/15	24/11	0.979/0.322[b]
APOE4 (±)	31/4	22/13	**6.293/0.012**[a,b]
Age	74.30 (5.63)	73.40 (6.85)	590.000/0.792[c]
Years of education	16.00 (2.32)	16.00 (2.58)	532.000/0.334[c]
Global Aβ	1.48 (0.17)	1.38 (0.14)	**424.000/0.027**[a,c]
CSF Aβ	648.33 (189.51)	705.30 (207.16)	568.000/0.758[c]
CSF t-tau	357.15 (123.76)	319.00 (130.35)	425.500/0.127[c]
CSF p-tau	33.75 (14.25)	30.40 (15.52)	438.000/0.174[c]
Regional Aβ	1.48 (0.17)	1.39 (0.13)	**401.000/0.013**[a,c]

Data are presented as mean (standard deviation) for continuous variables or frequencies for categorical ones.
Key: Aβ, amyloid-beta; CSF, cerebrospinal fluid; P-tau, Phospho-tau; T-tau, Total-tau.
[a] $p < 0.05$.
[b] Test stats refer to Pearson's chi-square.
[c] Test stats refer to Mann-Whitney's U.

Table A2
Final model summary of multinomial logistic regression analysis for variables predicting fast and slow progression in the CN-MCI/AD group

	Predictor	B	SE	Wald/*p*	Exp(B)	df	95% CI
Fast P.							
	Age	.341	.134	6.531/0.011	1.407	1	1.083-1.828
	Regional Aβ	5.626	2.097	7.198/0.007	277.670	1	4.555-16926.470
	Intercept	-31.130	11.714	7.063/0.008	-	1	-
Slow P.							
	APOE4 (0)	-2.693	1.160	5.389/0.020	0.068	1	0.007-0.657
	Intercept	-2.826	9.781	0.083/0.773	-	1	-
			Nagelk. R^2	PAC	X^2	*p*	*Df*
Overall model evaluation			0.572	74.5	38.068	18	0.004

Table A3
Final model summary of multinomial logistic regression analysis for variables predicting fast and slow progression in the MCI-AD group

	Predictor	B	SE	Wald/*p*	Exp(B)	df	95% CI
Fast P.							
	Regional Aβ	8.287	4.314	3.691/0.005	500095.51	1	53.170–8924841576
	Sex (0)	-0.178	0.571	0.098/0.031	0.241	1	0.067–0.877
	APOE4 (0)	0.423	0.548	0.596/0.026	0.163	1	0.033–0.802
	Intercept	-17.864	5.306	11.335/0.001	-	1	-
			Nagelk. R^2	PAC	X^2	*p*	*Df*
Overall model evaluation			0.385	63.6	57.095	0.000	18

MCI-AD progressors, and the initial 104 stables from the MCI-MCI group. Ultimately, multinomial logistic regression analyses between the slow and fast progressor groups were performed, respectively, with the stable groups serving as reference group. The same independent variables as in the previous analyses were included in both models, next to the identified brain regions from the respective analysis.

Fast and slow CN-MCI/AD progressors were on average similar in years of education, APOE4 carriership, ratio of females to males, global and regional Aβ burden, and all of the CSF biomarkers. Fast CN-MCI/AD progressors had a higher age than slow progressors (Table A1). Fast and slow MCI-AD progressors were on average similar in years of age, education, ratio of females to makes, and all of the CSF biomarkers. Fast MCI-AD progressors had a higher global and regional Aβ burden and a positive APOE4 carriership than slow MCI-AD progressors (Table A1).

For the CN-MCI/AD analysis, fifteen fast progressors, 12 slow progressors, and 28 stables were included in the multinomial logistic regression analysis due to missing data. For the MCI-AD analysis, 35 fast progressors, 35 slow progressors, and 104 stables were included in the analysis. Preliminary results on factors contributing to the rate of progression indicated that higher age and regional Aβ contribute to progression from CN to MCI or AD within 36 months after establishment of amyloid positivity. For slow progression from CN to MCI or AD, there was an association with a positive APOE4 carriership (Table A2). Similarly, higher regional Aβ, as well as being female and an APOE4 carrier contribute to progression from MCI to AD within 12 months after establishment of amyloid positivity. None of the variables were able to predict slow progression, however, regional Aβ was trend significant ($p = 0.055$).

Table A3

Results of the multinomial logistic regression analysis in the CN-MCI/AD group with the stable group (CN-CN) serving as reference group. Only significant results are reported. Abbreviations: CI, confidence interval; df, degrees of freedom; PAC, percentage accuracy in classification for the whole sample; SE, standard error. Sex coded as 0 for male and 1 for female; APOE4 carriership coded as 0 for negativity and 1 for positivity.

Results of the multinomial logistic regression analysis with the stable group (CN-CN) serving as reference group. Only significant results are reported. Abbreviations: CI, confidence interval; df, degrees of freedom; PAC, percentage accuracy in classification for the whole sample; SE, standard error. Sex coded as 0 for male and 1 for female; APOE4 carriership coded as 0 for negativity and 1 for positivity.

Appendix B

B1. Sensitivity analysis

Due to the already limited dataset in the CN-CN and CN-MCI/AD groups, participants were, this time, not matched based

Table B1
Mean and standard deviations per group for the sensitivity analysis

Variable	CN-CN(N = 30)	CN-MCI/AD(N = 21)	MCI-MCI(N = 47)	MCI-AD(N = 47)
Age (years)	76.71 ± 4.85	77.94 ± 4.82	71.79 ± 5.64	72.00 ± 5.75
Sex (m/f)	17/13	11/10	27/20	27/20
APOE4 (±)	7/23	9/12	28/19	35/12
Education (years)	16.60 ±2.25	16.29 ± 2.89	15.87 ± 2.77	15.83 ± 2.75
Months stable	70.4 ± 17.18	20.00 ± 10.62	64.60 ± 13.60	24.26 ± 8.10
CSF Aβ	1001.95 ± 408.46 (24)	879.68 ± 382.40 (15)	805.31 ± 300.62 (38)	675.25 ± 178.64 (45)
CSF t-tau	310.09 ± 138.31 (24)	306.54 ± 102.79 (15)	275.09 ± 94.58 (42)	416.45 ± 138.36 (45)
CSF p-tau	29.88 ± 14.59 (24)	30.02 ± 11.86 (15)	26.23 ± 10.39 (42)	43.11 ± 15.56 (45)
Global Aβ	1.25 ± 0.20	1.55 ± 0.28	1.23 ± 0.16	1.49 ± 0.13

Values are given as mean ± standard deviation. Values in brackets are number of included datapoints if data was missing.
Key: APOE4, Apolipoprotein E4; CN-CN, cognitively normal stable; CN-MCI/AD, cognitively normal progressed to MCI or AD; MCI-MCI, mild cognitive impairment stable; MCI-AD, mild cognitive impairment progressed to AD.

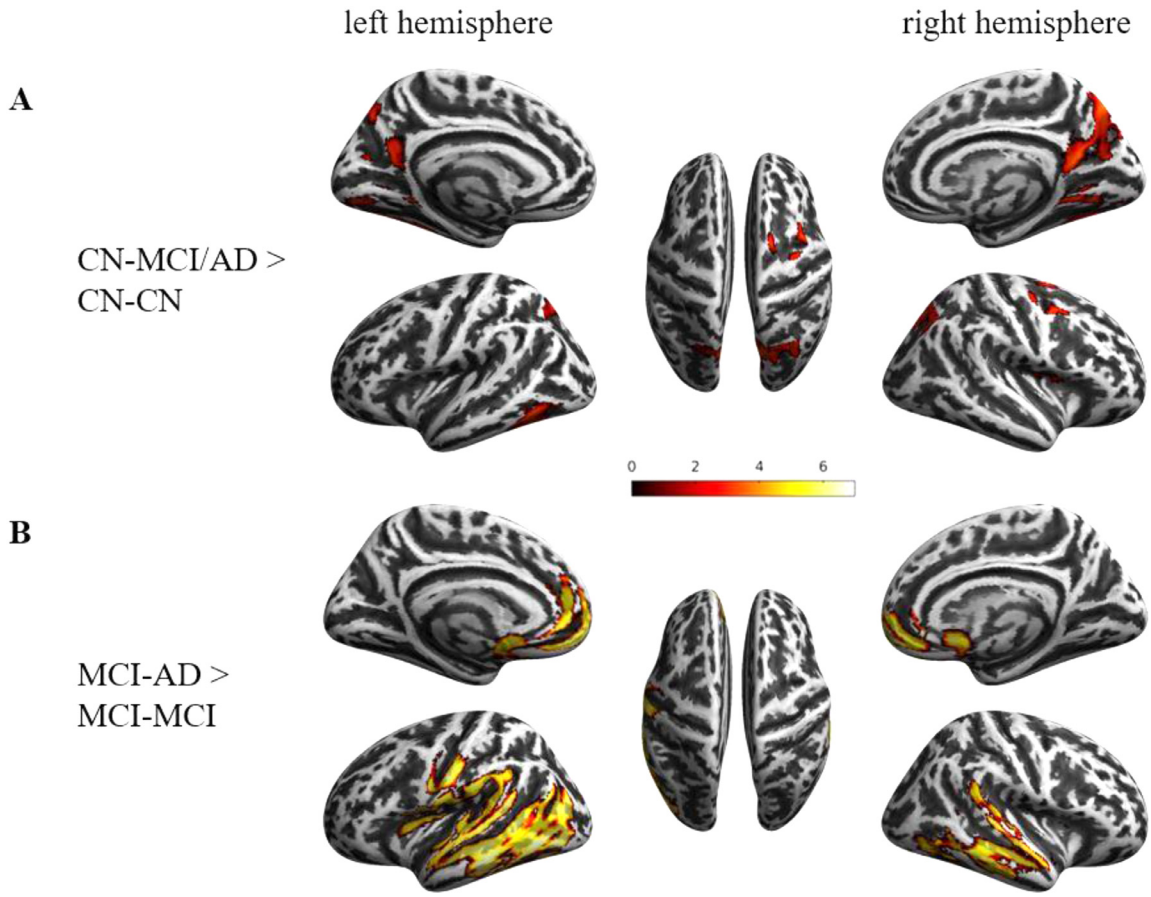

Figure B1. Regional differences in Aβ burden for the sensitivity analysis. (A) Regional differences in Aβ burden for CN-MCI/AD (N = 30) > CN-CN (N = 21), and (B) MCI-AD (N = 47) > MCI-MCI (N = 47). Results are color-coded according to the t-value statistics and illustrated on an inflated representation of the brain using CAT12 toolbox.

Table B2
Binary logistic regression analysis for variables predicting progression from CN to MCI or AD and from MCI to AD

	Predictor	β	SE β	Wald's X^2	*Df*	*P*	e^{β}	95% CI e^{β}
CN-CN versus	Constant	-30.138	13.859	4.729	1	0.030	0.000	-
CN-MCI/AD	Regional Aβ	10.290	4.372	5.540	1	0.019	29432.965	5.594–154851292
	Age	0.390	0.172	5.169	1	0.023	1.477	1.055–2.068
MCI-MCI versus	Constant	-14.431	5.961	5.862	1	0.015	0.000	-
MCI-AD	CSF Aβ	-0.004	0.002	3.827	1	0.050	0.996	0.993–1.000
	Regional Aβ	17.406	7.546	5.321	1	0.021	36268952	13.694-9.606E+13
	Test			X^2	*df*	*p*	Nagelk. R^2	**PAC**
CN-CN versus	Overall model evaluation			23.652	9	0.005	0.618	87.2
CN-MCI/AD	Goodness-of-fit test			12.922	8	0.115	-	-
MCI-MCI versus	Overall model evaluation			52.746	9	0.000	0.629	86.7
MCI-AD	Goodness-of-fit test			2.468	8	0.963	-	-

All predictor variables that showed non-significant associations were omitted from the table.
Key: e^{β}, odds ratio. CI, confidence interval.

on age and sex. However, it was ensured that the groups did not differ significantly on these variables. Given the large sample size of the MCI-MCI/MCI-AD groups, participants in the MCI-MCI and MCI-AD groups were matched on age and sex. This resulted in a final dataset of 30 CN-CNs, 21 CN-MCI/ADs, and 47 MCI-MCIs and MCI-ADs, respectively (Table B1). Similar to the previous analyses, 2-sample t-tests were performed with APOE4 carriership as covariate and a brain mask of the AAL atlas excluding the cerebellum. Significant regions were extracted and the overall mean across regions was computed. Binary logistic regression analyses were performed including all previously mentioned variables and the extracted mean SUVRs of the identified regions.

The CN-CN and CN-MCI/AD groups differed only significantly on baseline global Aβ ($p = 0.003$). The MCI-MCI and MCI-AD groups differed on baseline global SUVR ($p < 0.001$), CSF t-tau ($p < 0.001$), and CSF p-tau ($p < 0.001$). The voxel-wise whole-brain analysis yielded higher regional differences in Aβ burden in the right and left precuneus and posterior cingulate gyrus, right putamen, angular gyrus, superior temporal gyrus, anterior and posterior insula, and right lingual gyrus for the CN-MCI/AD group compared to the CN-CN group ($p < 0.001$, uncorrected, Figure B1[A]). None of the clusters in this comparison survived correction for multiple comparisons. Regional differences in Aβ burden was also higher in the right and left anterior cingulate cortex, middle and inferior temporal gyrus, superior frontal gyrus, putamen, caudate, pallidum, left

posterior cingulate gyrus, angular gyrus, central operculum, inferior occipital gyrus, middle and inferior occipital gyrus, basal forebrain and frontal pole, as well as right medial frontal cortex for the MCI-AD group compared to the MCI-MCI group (FWE-corrected, Figure B1[B]). The binary logistic regression analysis for the CN-CN and CN-MCI/AD groups showed that the mean regional SUVR was significant in the model together with age, ($X^2(9) = 23.652$, $p < 0.005$). The model explained 61.8% of variance and correctly classified 87.2% of cases (Table B2). Similarly, the mean regional SUVR was also significant in the binary logistic regression analysis of the MCI-MCI and MCI-AD groups together with CSF Aβ, ($X^2(9) = 52.746$, $p < 0.000$). The model explained 62.9% of variance and correctly classified 86.7% of cases (Table B2).

Appendix C

Table C1 and C2.

Table C1
Binary logistic regression analysis CN-CN versus CN-MCI/AD

	B	S.E.	Wald	df	*p*	Exp(B)
Age	0.145	0.080	3.253	1	0.071	1.156
Sex (1)	-1.089	0.902	1.458	1	0.227	0.337
Education	-0.057	0.165	0.120	1	0.729	0.945
APOE4 (1)	-1.556	0.797	3.811	1	0.051	0.211
CSF amyloid	-0.002	0.001	1.739	1	0.187	0.998
CSF t-tau	0.028	0.020	1.933	1	0.164	1.028
CSF p-tau	-0.256	0.185	1.914	1	0.166	0.774
Global amyloid	0.002	2.259	0.000	1	0.999	1.002
Regional amyloid	5.013	1.865	7.221	1	0.007[a]	150.333
Constant	-15.390	7.833	3.860	1	0.049	0.000

Sex coded as 1 = male and 2 = female; APOE4 carriership coded as 1 = negative and 2 = positive.
[a] $p < .005$

Table C2
Binary logistic regression analysis MCI-MCI versus MCI-AD

	B	S.E.	Wald	df	*p*	Exp(B)
Age	0.031	0.033	0.875	1	0.350	1.031
Sex (1)	-0.675	0.438	2.375	1	0.123	0.509
Education	0.084	0.071	1.398	1	0.237	1.087
APOE4 (1)	-0.112	0.442	0.064	1	0.800	0.894
CSF amyloid	-6.409	3.425	3.501	1	0.061	0.002
CSF t-tau	-0.002	0.001	4.731	1	0.030[a]	0.998
CSF p-tau	-0.002	0.006	0.141	1	0.708	0.998
Global amyloid	0.065	0.058	1.248	1	0.264	1.067
Regional amyloid	9.834	3.551	7.670	1	0.006[a]	18650.596
Constant	-7.347	3.111	5.577	1	0.018	0.001

Sex coded as 1 = male and 2 = female; APOE4 carriership coded as 1 = negative and 2 = positive.
[a] $p < 0.005$.

References

Albert, MS, DeKosky, ST, Dickson, D, Dubois, B, Feldman, HH, Fox, NC, Gamst, A, Holtzman, DM, Jagust, WJ, Petersen, RC, Snyder, PJ, Carrillo, MC, Thies, B, Phelps, CH, 2011. The diagnosis of mild cognitive impairment due to Alzheimer's disease: recommendations from the National Institute on Aging-Alzheimer's Association workgroups on diagnostic guidelines for Alzheimer's disease. Alzheimers Dement 7 (3), 270. doi:10.1016/j.jalz.2011.03.008.

Bateman, RJ, Xiong, C, Benzinger, TLS, Fagan, AM, Goate, A, Fox, NC, Marcus, DS, Cairns, NJ, Xie, X, Blazey, TM, Holtzman, DM, Santacruz, A, Buckles, V, Oliver, A, Moulder, K, Aisen, PS, Ghetti, B, Klunk, WE, McDade, E, Martins, RN, Masters, CL, Mayeux, R, Ringman, JM, Rossor, MN, Schofield, PR, Sperling, RA, Salloway, S, 2012. Morris JC for the dominantly Inherited Alzheimer network, 2012. Clinical and biomarker changes in dominantly inherited Alzheimer's disease. NEJM 369 (9), 795–804. doi:10.1056/NEJMoa1202753.

Bischof, GN, Jacobs, HIL, 2019. Subthreshold amyloid and its biological and clinical meaning. Neurology 93 (2), 72–79. doi:10.1212/WNL.0000000000007747.

Cho, H, Choi, JY, Hwang, MS, Kim, YJ, Lee, HM, Lee, JS, Lee, JH, Ryu, YH, Lee, MS, Lyoo, CH, 2016. In vivo cortical spreading pattern of tau and amyloid in the Alzheimer disease spectrum. Ann Neurol 80 (2), 247–258. doi:10.1002/ana.24711.

Ciarmiello, A, Tartaglione, A, Giovannini, E, Riondato, M, Giovacchini, G, Ferrando, O, De Biasi, M, Passera, C, Carabelli, E, Mannironi, A, Foppiano, F, Alfano, B, Mansi, L, 2019. Amyloid burden identifies neuropsychological phenotypes at increased risk of progression to Alzheimer's disease in mild cognitive impairment patients. Eur J Nucl Med Mol Imaging 46, 288–296. doi:10.1007/s00259-018-4149-2.

Corrada, MM, Brookmeyer, R, Paganini-Hill, A, Berlau, D, Kaway, CH, 2010. Dementia incidence continues to increase with age in the oldest old: the 90+ study. Ann Neurol 67 (1), 114–121. doi:10.1002/ana.21915.

Craft, S, Teri, L, Edland, SD, Kukull, WA, Schellenberg, G, McCormick, WC, Bowen, JD, Larson, EB, 1998. Accelerated decline in apolipoprotein E-epsilon4 homozygotes with Alzheimer's disease. Neurology 51 (1), 149–153. doi:10.1212/wnl.51.1.149.

Fagan, AM, Mintun, MA, Mach, RH, Lee, SY, Dence, CS, Shah, AR, LaRossa, GN, Spinner, ML, Klink, WE, Mathis, CA, DeKosky, ST, Morris, JC, Holtzman, DM, 2006. Inverse relation between in vivo amyloid imaging load and cerebrospinal fluid $Abeta_{42}$ in humans. Ann Neurol 59 (3), 512–519. doi:10.1002/ana.20730.

Fagan, AM, Mintun, MA, Shah, AR, Aldea, P, Roe, CM, Mach, RH, Marcus, D, Morris, JC, Holtzman, DM, 2009. Cerebrospinal fluid tau and $ptau_{181}$ increase with cortical amyloid deposition in cognitively normal individuals: Implications for future clinical trials of Alzheimer's disease. EMBO Mol Med 1 (8-9), 371–380. doi:10.1002/emmm.200900048.

Farrell, ME, Chen, X, Rundle, MM, Chan, MY, Wig, GS, Park, DC, 2018. Regional amyloid accumulation and cognitive decline in initially amyloid-negative adults. Neurology 91 (19), e1809–e1821. doi:10.1212/WNL.0000000000006469.

Ferreira, D, Rivero-Santana, A, Perestelo-Pérez, L, Westman, E, Wahlund, LO, Sarría, A, Serrano-Aguilar, P, 2014. Improving CSF biomarkers' performance for predicting progression from mild cognitive impairment to Alzheimer's disease by considering different confounding factors: A meta-analysis. Front Aging Neurosci 6, 287. doi:10.3389/fnagi.2014.00287.

Frings, L, Hellwig, S, Spehl, TS, Bormann, T, Buchert, R, Vach, W, Minkova, L, Heimbach, B, Klöppel, S, Meyer, PT, 2015. Asymmetries of amyloid-β burden and neuronal dysfunction are positively correlated in Alzheimer's disease. Brain 138, 3089–3099. doi:10.1093/brain/awv229.

Frisoni, GB, Govoni, S, Geroldi, C, Bianchetti, A, Calabresi, L, Franceschini, G, Trabucchi, M, 1995. Gene dose of the ε4 allele of apolipoprotein E and disease progression in sporadic late-onset Alzheimer's disease. Ann Neurol 37, 596–604. doi:10.1002/ana.410370509.

Guo, T, Landau, SM, Jagust, WJ, 2020. Detecting earlier stages of amyloid deposition using PET in cognitively normal elderly adults. Neurology 94 (14), e1512–e1524. doi:10.1212/WNL.0000000000009216.

Grothe MJ, Barthel H, Sepulcre J, Dyrba M, Sabri O, Teipel SJ, for the Alzheimer's Disease Neuroimaging Initiative, 2017. In vivo staging of regional amyloid deposition. AAN 89, 2031-2038. doi:10.1212/WNL.0000000000004643.

Hanseeuw, BJ, Betensky, RA, Mormino, EC, Schultz, AP, Sepulcre, J, Becker, JA, Jacobs, HIL, Buckley, RF, LaPoint, MR, Vannini, P, Donovan, NJ, Chhatwal, JP, Marshall, GA, Papp, KV, Amariglio, RE, Rentz, DM, Sperling, RA, Johnson, KAHarvard Aging Brain Study, 2018. PET staging of amyloidosis using striatum. Alzheimers Dement 14 (10), 1281–1292. doi:10.1016/j.jalz.2018.04.011.

Hirono, N, Hashimoto, M, Yasuda, M, Kazui, H, Mori, E, 2003. Accelerated memory decline in Alzheimer's disease with apolipoprotein epsilon4 allele. J Neuropsychiatry Clin Neurosc 15 (3), 354–358. doi:10.1176/jnp.15.3.354.

Jack Jr, CR, Albert, MS, Knopman, DS, McKhann, GM, Sperling, RA, Carrillo, MC, Thies, B, Phelps, CH, 2011. Introduction to the recommendations from the National Institute on Aging-Alzheimer's Association workgroups on diagnostic guidelines for Alzheimer's disease. Alzheimers Dement 7 (3), 257–262. doi:10.1016/j.jalz.2011.03.004.

Jun, S, Heeyoung, K, Bum Soo, K, Bong-Goo, Y, Won Gu, L, Alzheimer's Disease Neuroimaging Initiative, 2019. Quantitative brain amyloid measures predict time-to-progression from amnestic mild cognitive impairment to Alzheimer's Disease. J Alzheimers Dis 70 (2), 477–486. doi:10.3233/jad-190070.

Kanekiyo, T, Xu, H, Bu, G, 2014. ApoE and Aβ in Alzheimer's disease: accidently encounters or partners? Neuron 81 (4), 740–754. doi:10.1016/j.neuron.2014.01.045.

Kleiman, T, Zdanys, K, Black, B, Rightmer, T, Grey, M, Garman, K, Macovoy, M, Gelernter, J, van Dyck, C, 2006. Apolipoprotein E epsilon4 allele is unrelated to cognitive or functional decline in Alzheimer's disease: retrospective and prospective analysis. Dement Geriatr Cogn Disord 22 (1), 73–82. doi:10.1159/000093316.

Landau S, Jagust W, 2015. Florbetapir processing methods [PDF file]. Berkeley, CA: Author. Retrieved 16.04.2021 from https://adni.bitbucket.io/reference/docs/UCBERKELEYAV45/ADNI_AV45_Methods_JagustLab_06.25.15.pdf.

Lin, KJ, Hsiao, IT, Hsu, JL, Huang, CC, Huang, KL, Hsieh, CJ, Wey, SP, Zen, TC, 2016. Imaging characteristics of dual-phase 18F-florbetapir (AV-45/amyloid) PET for the concomitant detection of perfusion deficits and beta-amyloid deposition in Alzheimer's disease and mild cognitive impairment. Eur J Nucl Med Mol Imaging 43 (7), 1304–1314. doi:10.1007/s00259-016-3359-8.

Mattsson, N, Palmqvist, S, Stomrud, E, Vogel, J, Oskar Hansson, O, 2019. Staging β-amyloid pathology with amyloid positron emission tomography. JAMA Neurol 76 (11), 1319–1329. doi:10.1001/jamaneurol.2019.2214.

McKhann, GM, Knopman, DS, Chertkow, H, Hyman, BT, Jack Jr, CR, Kawas, CH, Klink, WE, Koroshetz, WJ, Manly, JJ, Mayeux, R, Mohs, RC, Morris, JC, Rossor, MN, Scheltens, P, Carrillo, MC, Thies, B, Weintraub, S, Phelps, CH, 2011. The diagnosis of dementia due to Alzheimer's disease: Recommendations from the National Institute on Aging-Alzheimer's Association workgroups on diagnostic guidelines for Alzheimer's disease. Alzheimers Dement 7, 263–269. doi:10.1016/j.jalz.2011.03.005.

Morris, JC, Roe, CM, Xiong, C, Fagan, AM, Goate, AM, Holtzman, DM, Mintun, MA, 2010. APOE predicts amyloid-beta but not tau Alzheimer pathology in cognitively normal aging. Ann Neurol 67 (1), 122–131. doi:10.1002/ana.21843.

Oulhaj, A, Wilcock, GK, Smith, D, de Jager, CA, 2009. Predicting the time of conversion to MCI in the elderly: role of verbal expression and learning. Neurology 73 (18), 1436–1442. doi:10.1212/WNL.0b013e3181c0665f.

Patterson, BW, Elbert, D, Mawuenyega, KG, Kasten, T, Ovod, V, Ma, S, Xiong, C, Chott, R, Yarasheski, K, Sigurdson, W, Zhang, L, Goate, A, Benzinger, T, Morris, JC, Holtzmann, D, Bateman, RJ, 2015. Age and amyloid effects on human CNS amyloid-beta kinetics. Ann Neurol 78 (3), 439–453. doi:10.1002/ana.24454.

Rowe, CC, Ellis, KA, Rimajova, M, Bourgeat, P, Pike, KE, Jones, G, Fripp, J, Tochon-Danguy, H, Morandeau, L, O'Keefe, G, Price, R, Raniga, P, Robins, P, Acosta, O, Lenzo, N, Szoeke, C, Salvado, O, Head, R, Martins, R, Masters, CL, Ames, D, Villemagne, VL, 2010. Amyloid imaging results from the Australian Imaging, Biomarkers and Lifestyle (AIBL) study of aging. Neurobiol Aging 31 (8), 1275–1283. doi:10.1016/j.neurobiolaging.2010.04.007.

Saint-Aubert, L, Barbeau, EJ, Péran, P, Nemmi, F, Vervueren, C, Mirabel, H, Payoux, P, Hitzel, A, Bonneville, F, Gramada, R, Tafani, M, Vincent, C, Puel, M, Dechaumont, S, Chollet, F, PAriente, J, 2013. Cortical florbetapir-PET amyloid load in prodromal Alzheimer's disease patients. EJNMMI Res 3, 43. doi:10.1186/2191-219X-3-43.

Sakr, FA, Grothe, MJ, Cavedo, E, Jelistratova, I, Habert, MO, Dyrba, M, Gonzalez-Escamilla, G, Bertin, H, Locatelli, M, Lehericy, S, Teipl, S, Dubois, B, Hampel, Hfor the INSIGHT-preAD study group & the Alzheimer Precision Medicine Initiative (APMI), 2019. Applicability of in vivo staging of regional amyloid burden in a cognitively normal cohort with subjective memory complaints: The INSIGHT-preAD study. Alzheimer's Res Ther. 11, 15. doi:10.1186/s13195-019-0466-3.

Sperling, RA, Aisen, PS, Beckett, LA, Bennett, DA, Craft, S, Fagan, AM, Iwatsubo, T, Jack Jr, CR, Kaye, J, Montine, TJ, Park, DC, Reiman, EM, Rowe, CC, Siemers, E, Stern, Y, Yaffe, K, Carrillo, MC, Thies, B, Morrison-Bohorad, M, Wagster, MV, Phelps, CH, 2011. Towards defining the preclinical stages of Alzheimer's disease: recommendations from the National Institute on Aging-Alzheimer's Association workgroups on diagnostic guidelines for Alzheimer's disease. Alzheimers Dement 7 (3), 280–292. doi:10.1016/j.jalz.2011.03.003.

Stern, Y, Brandt, J, Albert, M, Jacobs, DM, Liu, X, Bell, K, Marder, K, Sano, M, Albert, S, Del-Castillo Casternada, C, Bylsma, F, Tycko, B, Mayeux, R, 1997. The absence of an apolipoprotein epsilon4 allele is associated with a more aggressive form of Alzheimer's disease. Ann Neurol 41, 615–620. doi:10.1002/ana.410410510.

Teipel, SJ, Kurth, J, Krause, B, Grothe, MJ, 2015. The relative importance of imaging markers for the prediction of Alzheimer's disease dementia in mild cognitive impairment – Beyond regression. Neuroimage Clin 8, 583–593. doi:10.1016/j.nicl.2015.05.006.

Thal, DR, Rüb, U, Orantes, M, Braak, H, 2002. Phases of A beta-deposition in the human brain and its relevance for the development of AD. Neurology 58 (12), 1791–1800. doi:10.1212/wnl.58.12.1791.

Tsutsui, Y, Awamoto, S, Himuro, K, Umezu, Y, Baba, S, Sasaki, M, 2018. Characteristics of smoothing filters to achieve the guideline recommended positron emission tomography image without harmonization. Asia Ocean J Nuc Med Biol 6 (1), 15–23. doi:10.22038/aojnmb.2017.26684.1186.